ANTIOXIDANTS & REDOX SIGNALING
Volume 11, Number 7, 2009

DOI: 10.1089/ars.2009.2614

Forum Original Research Communication

Axonal Mitochondrial Clusters Containing Mutant SOD1 in Transgenic Models of ALS

Jose R. Sotelo-Silveira,[1,2,5] Paola Lepanto,[1] Victoria Elizondo,[1] Sofia Horjales,[2] Florencia Palacios,[2] Laura Martinez-Palma,[1] Monica Marin,[2] Joseph S. Beckman,[3] and Luis Barbeito[1,4]

Abstract

We studied the subcellular distribution of mitochondria and superoxide dismutase-1 (SOD1) in whole mounts of microdissected motor axons of rats expressing the ALS-linked SOD1-G93A mutation. The rationale was to determine whether physical interactions between the enzyme and mitochondria were linked to the axonopathy of motor fibers occurring in amyotrophic lateral sclerosis (ALS). Mitochondria and SOD1 displayed a homogeneous distribution along motor axons both in nontransgenic rats and in those overexpressing wild-type SOD1. In contrast, axons from SOD1-G93A rats (older than 35 days) showed accumulation of mitochondria in discrete clusters located at regular intervals. Most of SOD1 immunoreactivity was enriched in these clusters and colocalized with mitochondria, suggesting a recruitment of SOD1-G93A to the organelle. The SOD1/mitochondrial clusters were abundant in motor axons but scarcely seen in sensory axons. Clusters also were stained for neuronal nitric oxide synthase, nitrotyrosine, and cytochrome *c*. The later also was detected surrounding clusters. Ubiquitin colocalized with clusters only at late stages of the disease. The cytoskeleton was not overtly altered in clusters. These results suggest that mutant SOD1 and defective mitochondria create localized dysfunctional domains in motor axons, which may lead to progressive axonopathy in ALS. *Antioxid. Redox Signal.* 11, 1535–1545.

Introduction

Dominant missense mutations in the gene for SOD1 are responsible for at least 20% of familial ALS cases (3, 28). Despite the ubiquitous expression of SOD1, mutations in this protein produce a disease that selectively affects upper and lower motor neurons (7). Aberrant oxidative chemistry, glutamate excitotoxicity (6, 17), mitochondria dysfunction (22), and mutant SOD1 aggregation are among different hypotheses that have been formulated to explain the toxic property of SOD1 mutations (31). In particular, abnormal accumulation of ALS-linked SOD1 mutations to mitochondria has been shown to induce organelle dysfunction and subsequent oxidative stress, which may trigger profound defects in neuronal physiology (23, 27, 35).

Regardless of the preferred hypothesis, axonopathy is an early event in ALS transgenic models. Pathology in ALS-transgenic animals is presented in a distal-to-proximal fashion, affecting the distal axonal territory and then the motor neuron perikaryon (13). In particular, axonal transport deficits have been implicated in early stages of the development (36, 37, 39), and abnormal neurofilament organization (15, 16, 24, 29) may play a role in axonal ALS pathology.

More recently, selective retrograde movement of mitochondria on SOD1-G93A motor neurons in culture was linked to perturbation of the anterograde component of fast axonal transport (11).

Because misfolded SOD1 associates with the cytoplasmic face of mitochondria (35), and this interaction likely affects several physiologic properties of mitochondria, including

[1]Department of Cell and Molecular Neurobiology, Instituto de Investigaciones Biologicas Clemente Estable, and [2]Department of Cell and Molecular Biology, Facultad de Ciencias, Montevideo, Uruguay.
[3]Environmental Health Sciences Center, Oregon State University, Corvallis, Oregon.
[4]Institut Pasteur de Montevideo, Montevideo, Uruguay.
[5]Present address of Dr. Sotelo-Silveira: Laboratory of Molecular Technology, ATP, SAIC-National Cancer Institute, Frederick, Maryland.

their axonal transport (reviewed in 12), we hypothesized that SOD1 mutations may disrupt the organelle number or distribution, in affected motor axons. Axons exhibit a highly specialized and unique architecture that might facilitate functional and physical interactions between mutant SOD1 and mitochondria. We attempted to demonstrate such discrete physical interactions by using microdissected whole-mount preparations followed by image analysis in motor and sensory axons. We report large mitochondria/SOD1 clusters selectively located in motor axons of mice and rats expressing SOD1-G93A, detected from early stages of the disease.

Materials and Methods

Isolation of axoplasmic whole mounts from spinal roots

Sprague–Dawley SOD1-G93A L26H rats were kindly provided by Dr. David S. Howland (Wyeth Research, Princeton, NJ) (17). Wild-type SOD1 rats were kindly provided by Dr. Pak Chen (Stanford University). SOD1-G93A transgenic mice were obtained from Jackson Laboratories. Animals were treated in accordance with the guidelines for Care and Use of Laboratory Animals established by the National Institutes of Health, and all protocols conducted with mice and rats were previously submitted to and approved by the National Committee for Animal Experimentation (CHEA). Animals were killed by using sodium pentobarbital (IP, 200 mg/kg), and when unresponsive, decapitation was performed. Lumbar spinal nerve roots (ventral or dorsal from the same segment) were dissected from 35-, 65-, and 90-day-old SOD1-G93A rats or non-transgenic control littermates. Nerve root/rootlet were suspended in a modified gluconate-substituted calcium-free Cortland salt solution (20, 32, 33) containing 132 m*M* Na-gluconate, 5 m*M* KCl, 20 m*M* HEPES, 10 m*M* glucose, 3.5 m*M* $MgSO_4$, and 2 m*M* EGTA, pH 7.2, and stored at 4°C. A nerve root/rootlet, of 3–5 mm in length, was immersed in a solution of 30 mM zinc acetate, 0.1 *M* Tricine; (Sigma, St. Louis, MO), pH 4.8, for 10 min and then placed in a 35-mm plastic culture dish containing 2 ml of 40 m*M* aspartic acid, 38.4 m*M* Tris, 1 m*M* NaN3, and 0.005% Tween 20, pH 5.5. This "axon-pulling" solution allows axoplasm to be transferred away from the myelin sheath. Isolated axoplasmic whole mounts were attached with the aid of eyebrow-hair tools (an eyebrow hair attached to the tip of a Pasteur pipette) to number 1 coverslips (Sigma, St. Louis, MO) coated with 1% 3-aminopropyltriethoxysilane (Polysciences, Warrington, PA) in ethanol. Axonal diameters range from 4 to 8 μm. A minimum of three animals for each age and a combination of antibodies were used. Reproducible results were obtained with animals from different collaborating laboratories.

Polyclonal antibodies against human SOD1

A polyclonal antibody against human SOD1 was developed in rabbits challenged against 50 μg of pure recombinant human SOD1 (provided by Dr. Beatriz Alvarez, Universidad de la Republica, Uruguay). The SOD was expressed in *E. coli* and purified as described in the literature (2). The γ-globulin fraction was obtained from the sera by ammonium sulfate precipitation and then purified with affinity chromatography on a column made by fixing recombinant human SOD1 to CNBr-activated Sepharose 4B (Pierce, Rockford, IL). The SOD1-specific γ-globulin fraction was eluted with 0.2 *M* glycine buffer (pH 2.5) plus 0.5 *M* NaCl. The specificity of the antibodies was assessed with Western blot and dot-blot analysis. Protein extracts were prepared by using a modification of reference (8). In brief, tissues were homogenized on

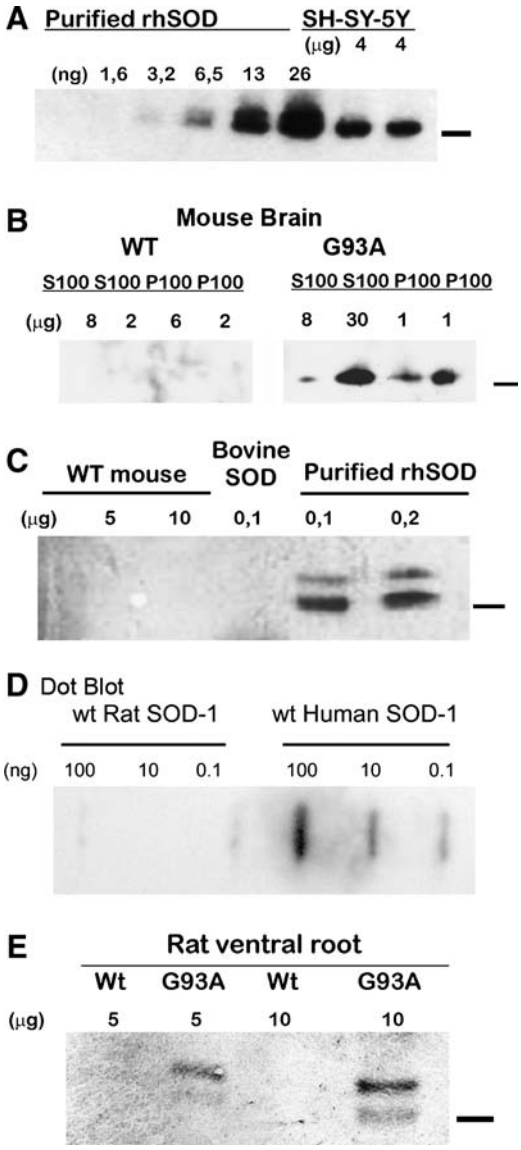

FIG. 1. Characterization of the antibody against human SOD1. Human, rat, mouse, and bovine protein extracts were used to demonstrate the specificity of antihuman SOD1 antibody after immunopurification in SDS-PAGE and dot blots. (**A**) The antibody recognized increasing concentrations of recombinant human SOD1 (rhSOD1) or protein extracts from human neuroblastoma cell line SH-SY-5Y. (**B**) The antibody recognized soluble and insoluble forms of human SOD1 from transgenic mice in pellets (P100) and supernatants (S100) from 100,000 g centrifugation extracts. (**C**) The antibody recognized recombinant human SOD1 but not commercial bovine SOD1. (**D**) Dot-blot with different concentrations of HPLC-purified wild-type rat and human SOD1 (0.1–100 ng). (**E**) Human SOD1 was detected specifically on ventral roots extracts. Bars to the right of Western blots indicate the 16.5-kDa molecular mass marker.

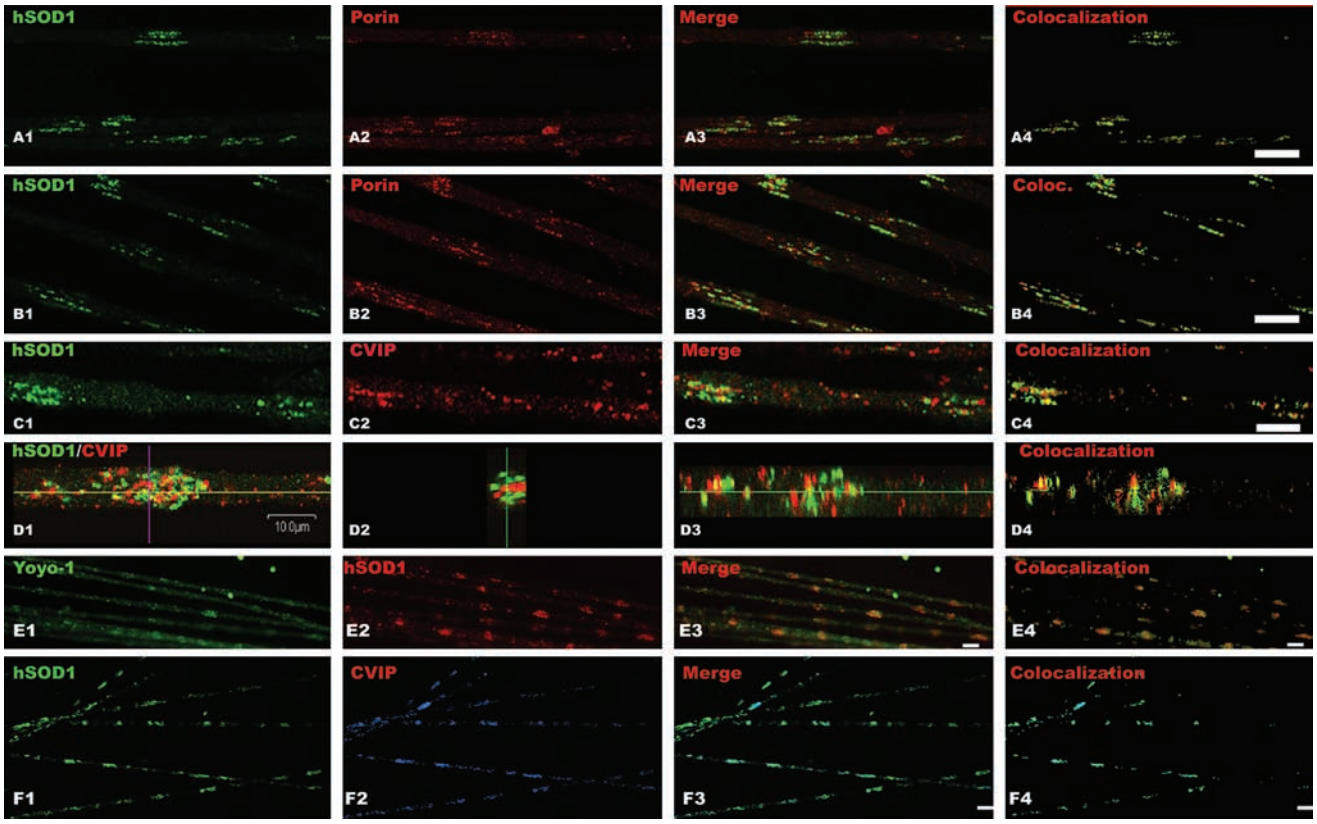

FIG. 2. Mitochondrial clusters colocalize with SOD1-G93A in motor axon of transgenic rats. Mitochondria and human SOD1 distribution in axons was analyzed in motor axonal whole mounts isolated from 65-day-old SOD1-G93A transgenic animals. Mitochondria were detected by using antibodies against porin, an outer-membrane protein, CVIP (complex five inhibitory protein), mitochondrial membrane protein, and YOYO-1 binding to mitochondrial nucleic acids. (**A**, **B**) Mitochondrial porin (red, **A2, B2**) and SOD1-G93A (green, **A1**, **B1**) staining in a single confocal section. Note the high degree of colocalization of both proteins in merged images (**A3**). (**B**) Areas in which mitochondria did not display SOD1 staining (red spots on merged image, **B3**). (**C**) CVIP immunoreactivity also showed clustering of mitochondria. (**C1**) Confocal section showing SOD1 staining; (**C**) CVIP staining; and (**C3**) merged images. (**D1**) Set of confocal images of the same focal plane for SOD1 and CVIP (human SOD1, green; CVIP, red). (**D2**) and (**D3**) are two different optical planes (blue line and yellow line of the axon visualized in **D1**) showing a large mitochondrial/SOD1 cluster. (**E**) DNA/RNA contents in clusters as showed by YOYO-1 staining (**E1**); (**E2**) human SOD1 immunoreactivity; (**E3**) merged image. (**F**) Mitochondria/SOD1 clusters in motor axons from SOD1-G93A mice. (**F1**) SOD1-G93A staining (green); (**F2**) CVIP staining, and (**F3**) merged image. Scale bars: for (**A**) to (**D**): 10 μm; (**E**) 5 μm; (**F**) 20 μm. The column to the right in each series shows green and red pixels that colocalize according to Costes criteria (see Materials and Methods). (For interpretation of the references to color in this figure legend, the reader is referred to the web version of this article at www.liebertonline.com/ars).

ice in lysis buffer (10% wt/vol) containing 50 m*M* Tris–HCl pH 7.5, 2 m*M* EGTA, 2 m*M* EDTA, 5 m*M* β-mercaptoethanol, 0.1 *M* NaCl, 100 μ*M* PMFS, 1 μg/ml leupeptin, 1 μg/ml apoprotinin) by using a Teflon-on-glass homogenizer and centrifuged at 15,000 *g* for 15 min at 4°C. Protein concentration was determined in the supernatant with BCA assay. A fraction of this supernatant was also used to prepare soluble (S100) or insoluble (P100) protein extracts by centrifugation at 100,000 *g* for 15 min at 4°C. Proteins were separated in 12% SDS-PAGE gels and transferred to a nitrocellulose membrane. Immunoblots were developed by using an HRP-labeled anti-rabbit antibody (Promega) and a chemoluminescence substrate Super signal Kit (Pierce, Rockford, IL).

The purified antibody was able to recognize either wild-type (natural or recombinant) or G93A mutant human SOD1 (Fig. 1A). No cross-reactivity was found against mouse, rat, or bovine SOD1 (Fig. 1C), tested in either different tissue lysates, HPLC-purified, or commercial protein. It did not recognize wild-type purified rat SOD1 in concentrations varying over two orders of magnitude (0.1–100 ng; Fig. 1D). When tested against soluble and insoluble SOD1, the antibody recognized only specific bands on extracts of transgenic animals carrying the SOD1-G93A, but not in extracts from control littermates (Fig. 1B). The antibody also recognized SOD1-G93A from ventral roots of transgenic animals as a double band (Fig. 1E), comparable to purified standard rhSOD1.

Immunofluorescence and confocal microscopy

Probes (YOYO-1, a high-affinity nucleic acid-binding dye), primary antibodies against Porin, complex five inhibitory protein (CVIP), and cytochrome *c*, and fluorescently conjugated secondary antibodies were obtained from Molecular Probes (Invitrogen, Carlsbad, CA). The other antibodies

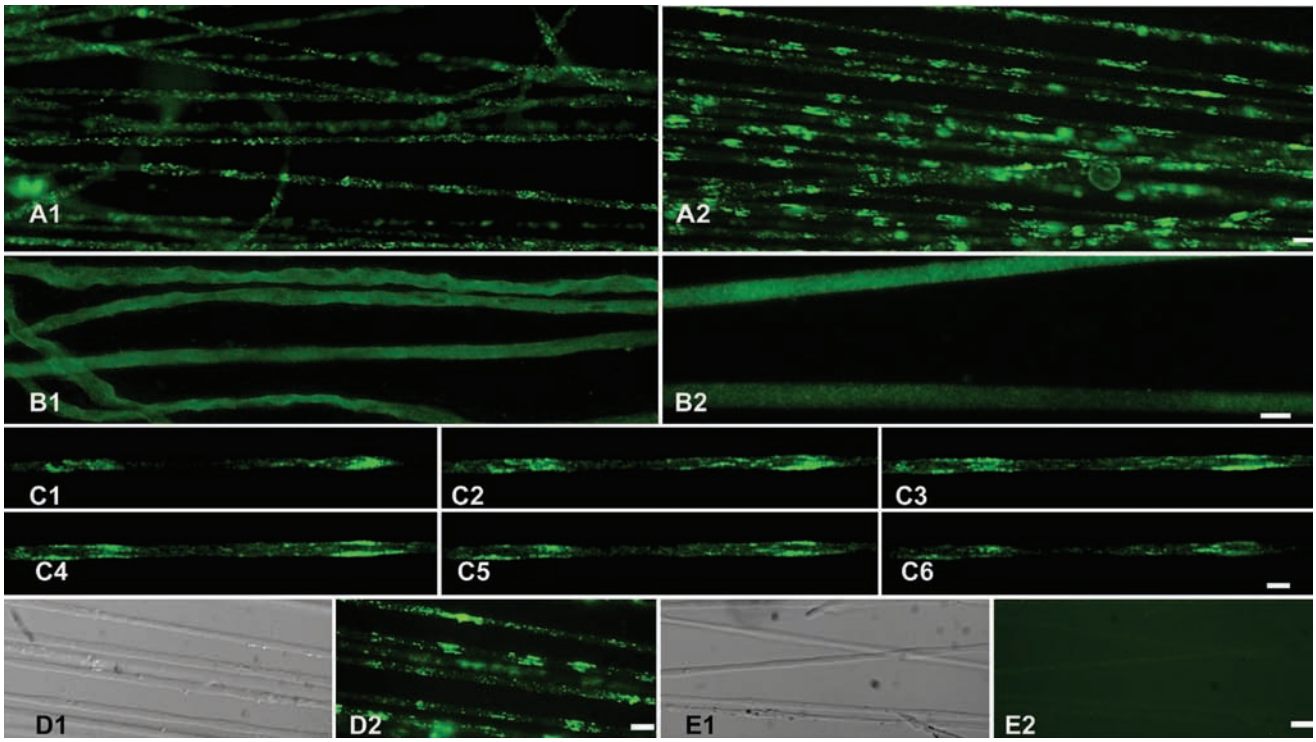

FIG. 3. Morphologic characterization of SOD1-G93A clusters in sensory and motor axons of asymptomatic rats. (**A1**) SOD1-G93A detected with immunofluorescence in lumbar sensory axons from 65-day-old SOD1-G93A rats. Note that no clusters were observed. (**A2**) SOD1-G93A detected in the ventral root at the same root level and from the same animal. Note the striking density of clusters. (**B**) Distribution of wild-type rat SOD1 in non-transgenic control littermates, as detected by using a panspecific anti-SOD1. (**B1**) Dorsal sensory axons; (**B2**) ventral motor axons. Note the homogeneous distribution of rat SOD1. (**C1–C6**) Six consecutive confocal images of 35-day-old SOD1-G93A motor axons showing SOD1 distribution through the axonal volume. (**D1**) Differential interference contrast (DIC) image; and (**D2**) SOD1-G93A staining of axons displaying clusters. Note that the affected axons were not morphologically altered. (**E1**) DIC image, and (**E2**) anti-human SOD1 staining of non-transgenic motor axons. Note the lack of immunoreactivity of rat SOD1. Scale bars: **A**, **D**, and **E**, 20 μm; **B** and **C**, 10 μm. (For interpretation of the references to color in this figure legend, the reader is referred to the web version of this article at www.liebertonline.com/ars).

used were the following: anti-nitrotyrosine (clone 1A6 and a rabbit polyclonal, both from Upstate-Millipore, Bedford, MA), nNOS, ubiquitin (Cell Signaling, Danvers, MA), panspecific anti-kinesin (clone IBII, Sigma, St. Louis, MO), anti-neurofilaments (heavy subunit; Sigma, St. Louis, MO), and a rabbit polyclonal specific for human SOD1 (ab52950; Abcam, Cambridge, MA).

Immunofluorescence was performed on axonal whole mounts, as previously reported (33). In brief, axons were blocked in 1% normal goat serum in PBS and then incubated for 1 h at room temperature with primary antibodies (at concentrations recommended by the manufacturer). After three washes with PBS (containing 0.01% of Tween), the secondary antibody was incubated for 45 min. Three final washes were performed before mounting the coverslips in 80% glycerol in phosphate buffer. Confocal and epifluorescence microscopy was performed with an Olympus Fluoview F300 mounted on a BX-51 microscope equipped with suitable lenses ($\times$40, 0.75 NA; $\times$60, 0.9 NA; $\times$100, 1.35 NA oil) and an Olympus DP70 digital camera. Images for WT SOD1-expressing animals were obtained with a Zeiss LSM510 Meta.

Quantitative imaging

Quantification of the number of clusters in ventral and dorsal axons was performed according to De Vos (11), with minor modifications. In brief, clusters between 4 and 7μm in length were counted in three animals in 200-μm axon segments of ventral and dorsal roots (in at least three different optical fields). The figures obtained were compared by using the *t* test, and the significance level used was $p < 0.001$ (pairs for comparisons detailed in the figure). Colocalization between mitochondrial markers and SOD1 or nitrotyrosine immunoreactivity and SOD1 was assessed by the method described by Costes *et al*. (9), implemented in the image-analysis software MIPAV (version 4.2.1) from the Center for Information Technology at NIH (25). In brief, this statistical approach quantifies automatically the amount of colocalization of two fluorescent-labeled proteins in an image, removing the bias of visual interpretation. The procedure determines simultaneously the maximal threshold of intensity for each color, below which pixels do not show statistical correlation. The pixels above the thresholds are used to create a mask showing colocalized signals depicted on the figures.

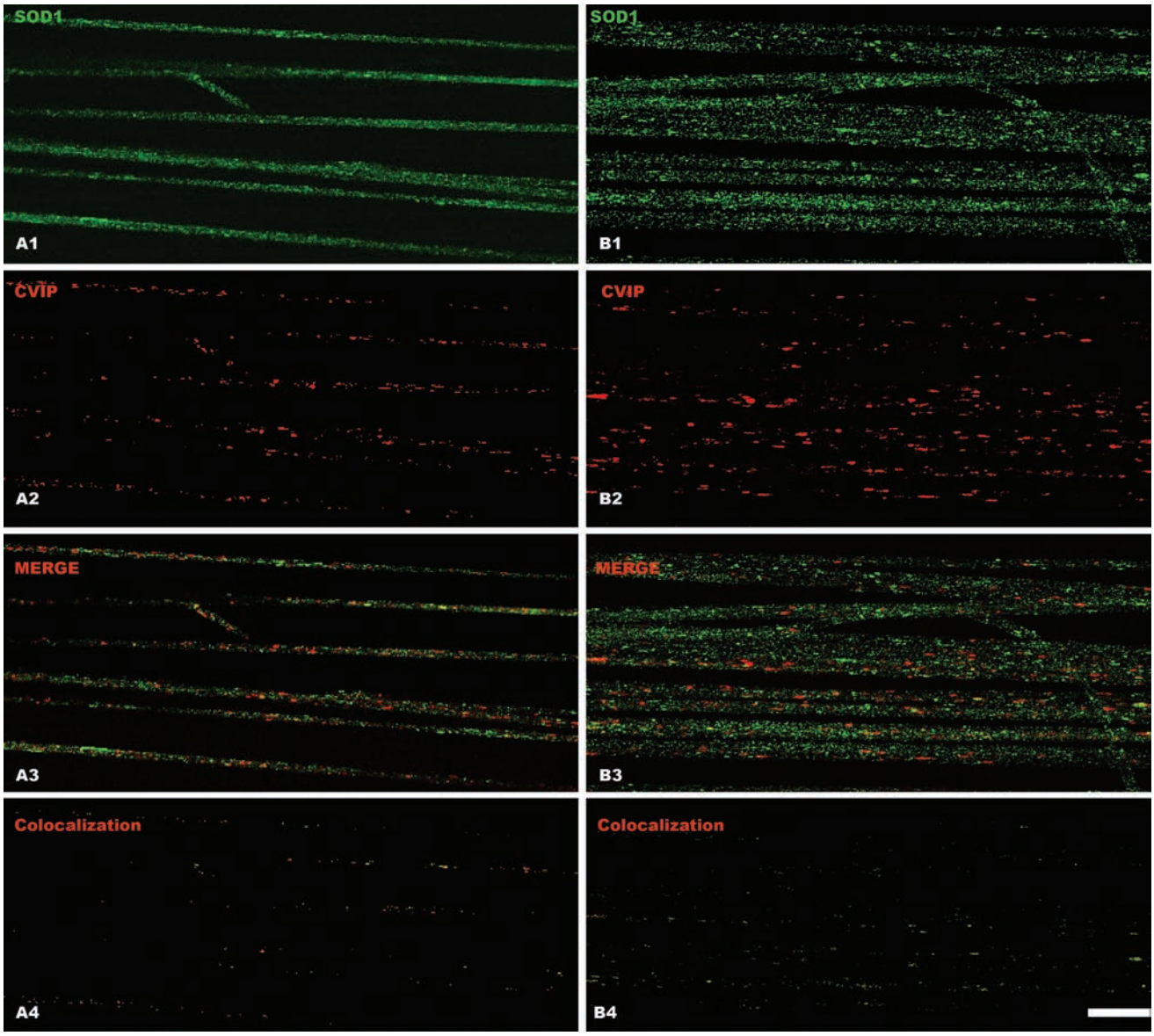

FIG. 4. Lack of mitochondria clustering in motor axons from rats overexpressing wild-type human SOD1. Motor axons were microdissected from 65-day-old rats overexpressing wild-type human SOD1 and stained to detect the human SOD1 protein (green) or CVIP mitochondrial protein (red). (**A1–4**) The signal obtained from a single confocal section of motor axons, whereas (**B1–4**) show a projection of multiple Z optical sections of several motor axons. Note the low degree of colocalization in (**A4**) and (**B4**), even when several optical sections were projected in the same plane (**B4**). Scale bar, 100 μm. (For interpretation of the references to color in this figure legend, the reader is referred to the web version of this article at www.liebertonline.com/ars).

Results

Mitochondrial clusters colocalize with SOD1-G93A in motor axons

Typically, mitochondria were distributed in large clusters in motor axons of presymptomatic (65 days old) SOD1-G93A rats (Fig. 2). When using our polyclonal antibody specific for human SOD1 (Fig. 1), we found that the majority of the signal was distributed along the axon in patches with the mitochondrial clusters (Fig. 2A4, B4, C4, and D1 to D4). SOD1 and mitochondrial clusters colocalized in most cases (Fig. 2; compare panels A4, B4, and C3), as suggested by Z projection of the cluster observed in panel D1. The observed clusters were usually localized in cortical areas of the axons (see confocal sections on Fig. 2A and B), but some clusters could be found in a central position (panel D). Furthermore, motor axons from transgenic SOD1-G93A mice displayed the SOD/mitochondria clusters identical to those in rats (Fig. 2F). The presence of clusters was observed in more than three animals at the specified ages, and clusters were confirmed by using a commercial antibody specific for human SOD1 (not shown). Quantification of pixel colocalization by means of the Pearson correlation coefficient (9) is shown in Fig. 2A4, B4, and C4. Analyzed in several fields, the Pearson correlation coefficient was between 0.65 and 0.8.

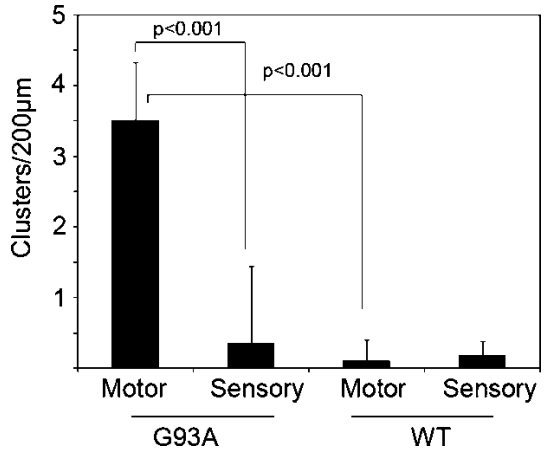

FIG. 5. Quantification of cluster density. Clusters were counted as described in Materials and Methods and expressed as number per the indicated axon segment. Note the difference between SOD1-G93A and wild-type SOD1 motor axons. The difference in cluster density between SOD1-G93A motor and sensory axons and WT SOD1 motor axons was statistically significant ($p < 0.001$) when the indicated pairs were compared. No difference was found between motor and sensory axons from WT hSOD1 animals. Error bars correspond to standard deviation (SD).

Clusters are observed at early stages of the disease

Clusters of SOD1 were observed in young animals, as early as 35-day-old rats (Fig. 3C; 2 months before disease onset) and up to 110 days old (not shown). The clusters in young animals were found mostly in cortical areas of the axon. It is worth noting that axons from symptomatic animals older than 120 days frequently break up in short segments when pulled.

Large clusters are not observed in dorsal root axons

Remarkably, the distribution of SOD1-G93A in dorsal roots was uniform with only few accumulations, which contrasted with numerous and large accumulations in the corresponding ventral root (Fig. 3, compare A2 with A1). The antibody against human SOD1 did not stain motor axons from non-transgenic littermates (Fig. 3E). Additionally, the endogenous, nonmutated rat SOD1 showed a uniform distribution with no accumulations in ventral root axons from non-transgenic animals (Fig. 3B1, B2).

Lack of mitochondrial clustering in motor axons from animal overexpressing wild-type SOD1

To determine whether mitochondria/SOD1 cluster formation was dependent on the G93A mutation, we analyzed axons prepared from rats that overexpressed the wild-type human SOD1. Both mitochondria and wild-type SOD1 showed a uniform distribution. Clusters were almost absent in these fibers (Fig. 4) with no apparent colocalization of SOD1 and mitochondria. Figure 4A1 to A4 clearly shows SOD1 distribution in a single confocal section, and panels B1 to B4 show a projection of optical sections in a single plane. The Pearson coefficient calculated in wild-type SOD1 axons was 0.35 or less as compared with 0.65 to 0.8 in those expressing SOD1-G93A.

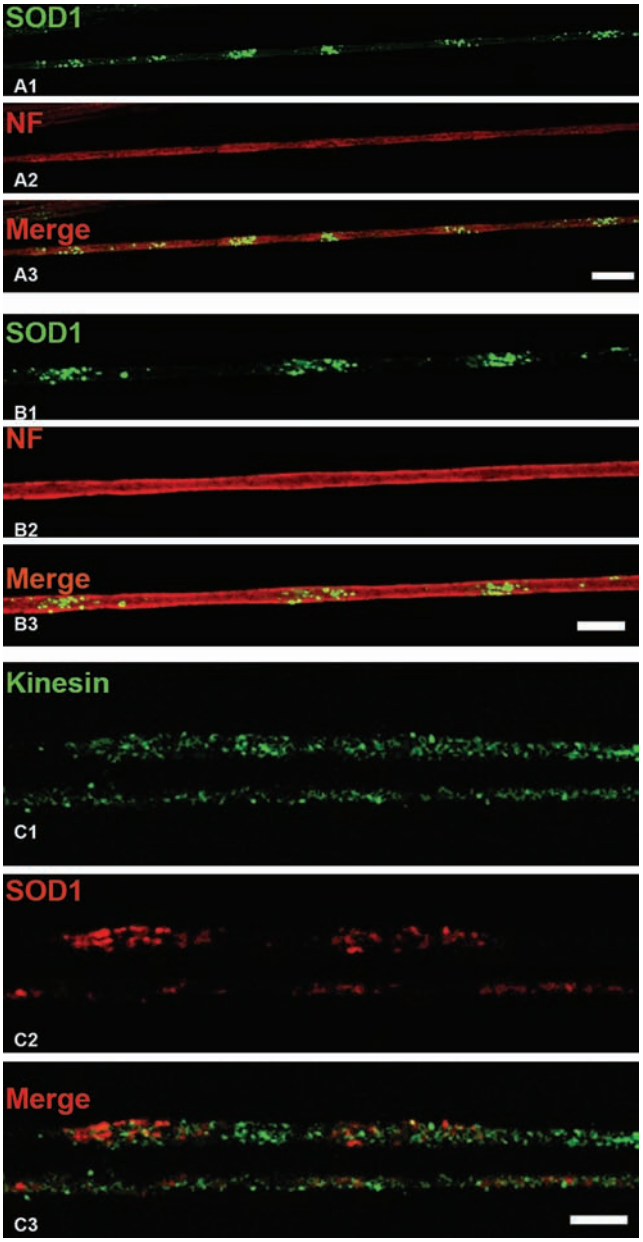

FIG. 6. Cytoskeletal and transport elements are distributed uniformly across SOD1 clusters. Motor axons from 65-day-old animals were dissected and stained to detect the mayor subunit of neurofilaments (NF) and kinesins I–II by using confocal microscopy. (**A, B**) NF-H staining in single confocal sections of two different areas at different magnifications. No major alterations are seen in areas of SOD1 clusters (green). Bars, 10 μm. (**C**) A portion of two motor axons is shown bearing an accumulation of SOD1-G93A but no colocalization with kinesin. In addition, the distribution of kinesin was not overtly altered in motor fibers. Scale bar, 10 μm. (For interpretation of the references to color in this figure legend, the reader is referred to the web version of this article at www.liebertonline.com/ars).

Quantification of cluster density between motor and sensory axons for both types of transgenic models is shown in Fig. 5. Clusters were observed in SOD1-G93A motor axons only, with an average of three to four clusters per axonal

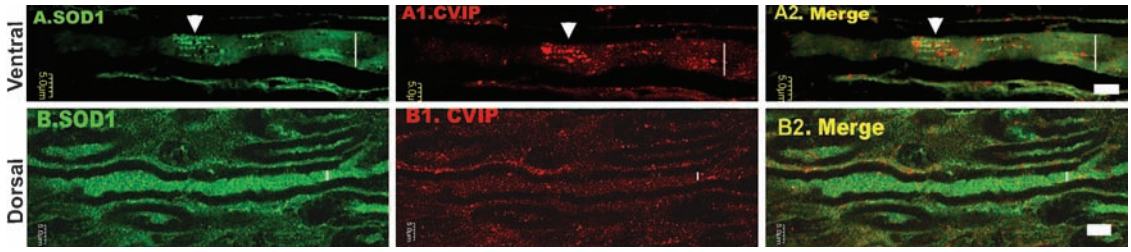

FIG. 7. Mitochondrial/SOD1 clusters are found in conventional tissue cryosections of the ventral root. The microphotographs shows 0.5-μm confocal sections of longitudinal cryosections of the roots stained with anti-human SOD1 (green) and CVIP (red). (**A**) and (**A2**) depict a myelinated axon from a ventral root (65-day-old SOD-G93A rat), where a cluster is indicated with an arrowhead. (**B**) to (**B2**) show a dorsal root where both mitochondria and SOD1 immunoreactivity were distributed evenly across the axons. Although SOD1-G93A was expressed in Schwann cells, no clusters were observed in these cells. Vertical bars, axon core. Scale bars, 5 μm. (For interpretation of the references to color in this figure legend, the reader is referred to the web version of this article at www.liebertonline.com/ars).

segment of ~200 μm. Wild-type SOD1-expressing animals did not show differential distribution of mitochondria between motor or sensory axons (Fig. 5).

Integrity of SOD1-G93A motor axons

Remarkably, the cylindrical morphology of axons was preserved in the SOD1-G93A rats, as observed in phase contrast and confocal microscopy (Fig. 3D). Immunostaining for neurofilaments (NF-H; Fig. 6A and B) or kinesin I-II (Fig. 6C) was performed to estimate the structural integrity of axons around the clusters. No overt alteration was noted in the distribution of both proteins along the SOD1-G93A motor axons. Furthermore, SOD1/mitochondrial clusters also were found in longitudinal cryosections of SOD1-G93A ventral roots as isolated formations (Fig. 7A, B).

Nitrotyrosine, cytochrome c*, and ubiquitin immunoreactivity in SOD1/mitochondrial clusters*

To determine whether mitochondria in clusters were functionally altered, we analyzed the distribution of cytochrome *c*, nitrotyrosine, and ubiquitin in axons from SOD1-G93A transgenic animals. Strikingly, cytochrome *c* was detected concentrated in mitochondria but also as diffuse

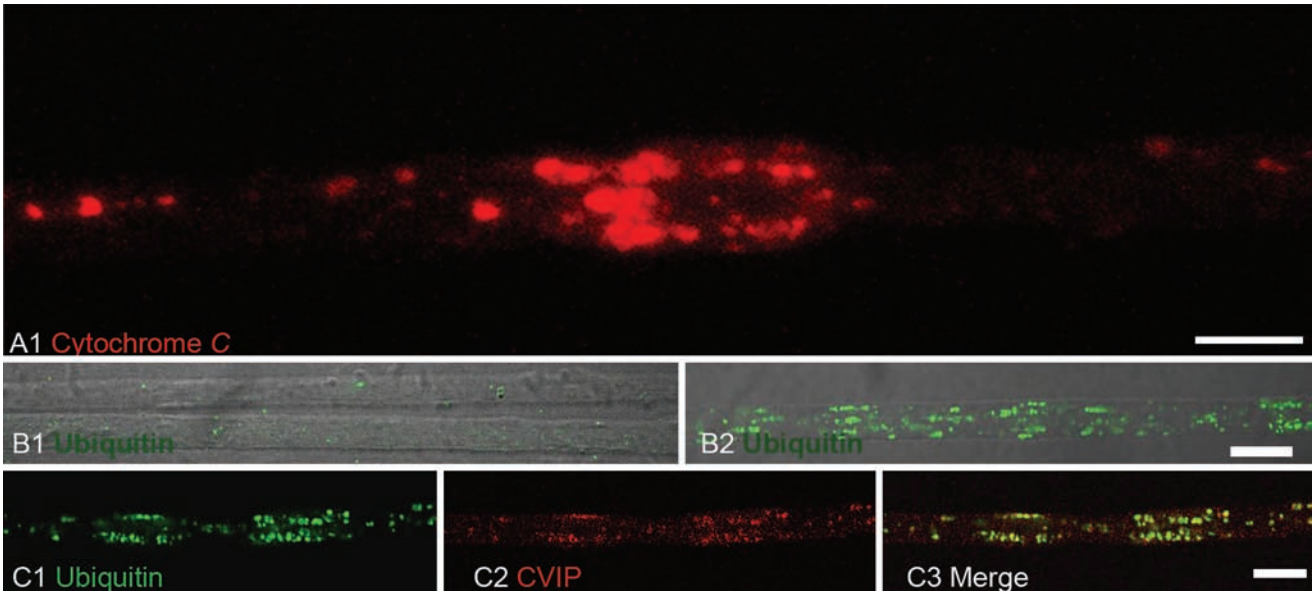

FIG. 8. Cytochrome *c* and ubiquitin immunoreactivity in motor axons from SOD1-G93A rats. (**A**) Cytochrome *c* (red) labelling followed the pattern of mitochondria distribution. Note the diffuse pattern of staining surrounding the mitochondria clusters, suggesting release of the protein due to organelle damage. (**B**) Comparison of ubiquitin immunoreactivity between 65-day-old axons (**B**) and 100-day-old axons (**B1**). In both cases, the image was obtained by merging DIC and confocal images. Bar, 10 μm. Note that ubiquitin staining in non-transgenic motor axons is comparable to that in 65-day-old SOD1-G93A rats. (**C**) Ubiquitin (green) was detected together with mitochondria (red) in a motor axon from a 110-day-old SOD1-G93A rat. Scale bars (**B**) and (**C**), 10 μm. (For interpretation of the references to color in this figure legend, the reader is referred to the web version of this article at www.liebertonline.com/ars).

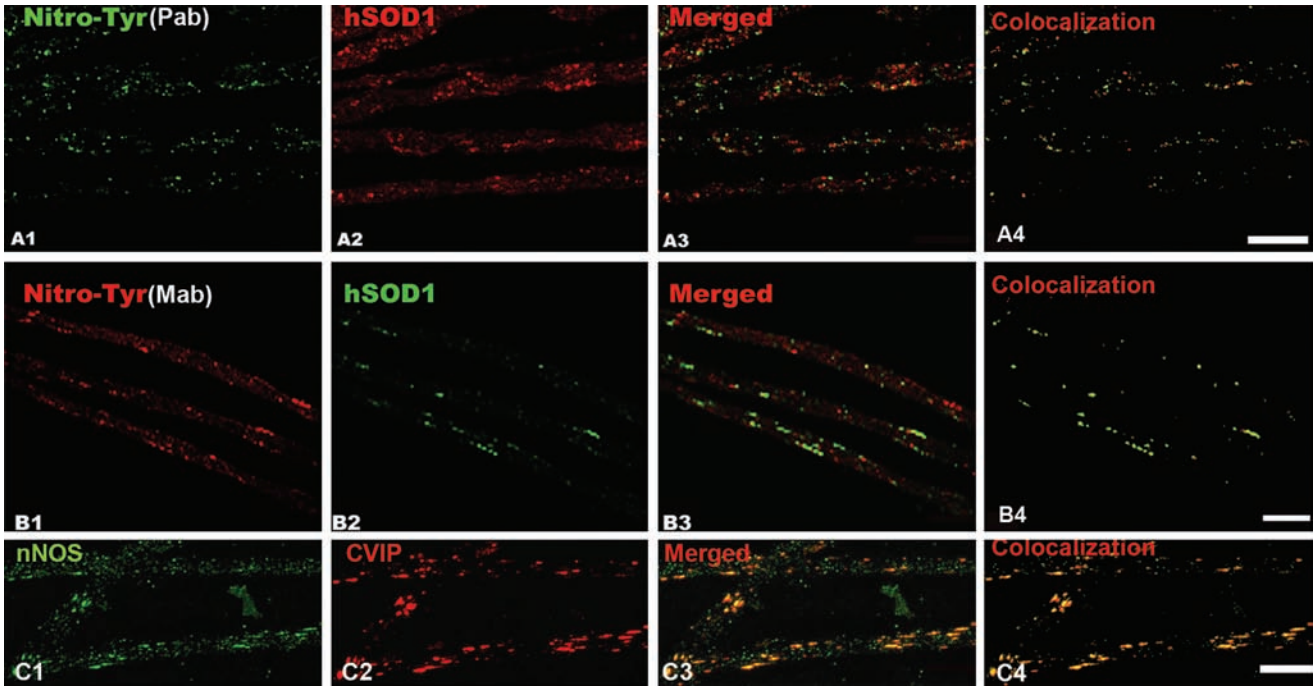

FIG. 9. Nitrotyrosine and NOS immunoreactivity in clusters of motor axons expressing SOD1-G93A. (**A**) Nitrotyrosine (**A1**, green) was detected with a polyclonal antibody and mitochondria by using CVIP antibody (**A2**, red). The merged image is seen in (**A3**). (**B**) Nitrotyrosine (**B1**, red) was detected with a monoclonal antibody (clone 1A6) and colocalized with SOD1-G93A (**B2**, green). The merged image is shown in (**B3**). (**C**) nNOS immunoreactivity (**C1**) colocalized with mitochondria (**C2,** CVIP). (**A4**), (**B4**), and (**C4**) show pixel colocalization masks obtained for each respective probe pair. In both cases, axons were microdissected from 65-day-old SOD1-G93A rats. Scale bars, 10 μm. (For interpretation of the references to color in this figure legend, the reader is referred to the web version of this article at www.liebertonline.com/ars).

staining surrounding them in 65-day-old or older axons, suggesting its release from mitochondria (Fig. 8A). Ubiquitin was detected in only late stages of the disease (100-day-old rats; Fig. 8B, C). We found that SOD1 clusters were immunoreactive to two different antibodies against nitrotyrosine (Fig. 9A and B) and to neuronal nitric oxide synthase (Fig. 9C) in axons from 65-day-old SOD1-G93A rats. These results suggest the formation of reactive species derived from nitric oxide, including peroxynitrite at mitochondrial clusters.

Discussion

We provide evidence of an abnormal distribution of mitochondria and mutant SOD1 in motor axons, forming a regular pattern of large clusters. Most likely, clustering would have escaped observation in conventional root cryosections that do not allow the analysis of long segments of axons in the same field. In addition, we show evidence that clustering is dependent on SOD1-G93A in motor axons, scarcely found in sensory axons, and appears early at asymptomatic stages of the disease. Colocalization of clusters with molecular markers such as ubiquitin, cytochrome *c*, nitrotyrosine, and nNOS allows us to suggest that mutant SOD1 and defective mitochondria create localized dysfunctional domains in motor axons, which may provide a clue to understanding progressive axonopathy in ALS.

Motor neurons are highly compartmentalized cells in which >95% of the cell volume is the axon (10). It might be possible that a yet-unknown feature of motor-axon architecture facilitates the previously reported physical interactions between mutated SOD1 and mitochondria (23, 27, 35). We attempted to demonstrate such discrete physical interactions by using whole-mount axoplasmic preparation, which was previously shown to provide detailed information of the subcellular localization of large molecules and organelles (20, 21, 32, 33). This technique allows the visualization of up to thousands of microns of linear axoplasm, preserving its structural features (21) and its functionality, when performed in non-denaturing conditions (19). However, the technique also may lead to potential artifacts. For this reason, we included different control experiments to confirm the occurrence of clustering. Thus, we show that clusters also can be found in conventional cryosections and are not associated with overt alteration of kinesin or NF-H distribution, as would be expected in an artifact condition. In addition, we found that SOD1/mitochondrial clustering in sensory axons was observed at very low frequency (Figs. 3A and 5), and absent from axons containing WT SOD1, suggesting an increased vulnerability of motor axons.

The characteristic diffuse staining of cytochrome *c* immunoreactivity surrounding the clusters suggests mitochondrial dysfunction. Cytochrome *c* released in the axoplasm might elicit local activation of proteolytic cascades similar to those triggering apoptosis in the neuronal perikaryon. The implication of such biochemical pathways in the axon compartment is presently unknown. In agreement, nNOS and nitrotyrosine

immunoreactivity were increased in axonal clusters, suggesting nitrative stress associated with dysfunctional mitochondria. Nitrotyrosine immunoreactivity in motor axons was previously reported in patients with sporadic ALS (1). In particular, the mitochondrial/SOD-cluster environment could facilitate the formation of neurotoxic Zn-deficient SOD1 species (5). Taken together, the characterization of clusters in motor axons indicates that mitochondria in clusters may become dysfunctional. Clusters may modify the function of restricted areas of the axoplasm, interfering, for example, with normal trafficking of organelles or trophic factors.

The SOD1 clusters in axons were preferentially localized in the axonal cortex in early stages and then invaded progressively the axonal core. This particular localization probably reflects the fact that clusters are displaced to the periphery of the axon, allowing the main axonal trafficking in the core. In addition, the increased binding of SOD1 to mitochondria in clusters seems to be specific for the SOD1-G93A mutation, because no evidence of preferential colocalization was observed for endogenous rat SOD1 and overexpressed wild-type human SOD1. Moreover, we provide evidence of a progressive ubiquitination of hSOD1/mitochondrial clusters, which becomes apparent in late stages of the disease. In agreement, previous reports showed increased levels of ubiquinated proteins in the sciatic nerve (14) and spinal cord of ALS mice (4).

Although SOD1 can accumulate in the mitochondrial matrix or interspace, it is likely that misfolded mutant SOD1 in clusters is preferentially associated with the outer membrane of mitochondria (35). These authors propose that increasing recruitment of SOD1 to the mitochondrial outer membrane will increase as the disease progresses. Thus, at early stages of the disease, mitochondria may depart to the axon from the cell body with minimal content of mutant SOD1 on its outer membrane. It should be established whether SOD1 progressively increases in the outer membrane of mitochondria as they move anterogradely into the axoplasm. It is likely that SOD1 mutations provoke defective mitochondria traffic in axons. Depolarized mitochondria have been reported to be preferentially transported anterogradely (26). In addition, *in vitro* experiments tracking mitochondria in neurons from SOD1-G93A animals reported selective reduction of anterograde transport (11), which may further reduce the number of axonal mitochondria.

The dynamics of the process of accumulation must be studied to establish whether mitochondria in clusters were being transported anterogradely or retrogradely. A recent study showed that in asymptomatic stages, at the ultrastructural level, mitochondria are accumulated in the axon hillock and initial segment (30). Interestingly, aggreosome formation (18) in culture cells expressing SOD1-G93A indicated that a tubulin minus end directed traffic of organelles ending in formation of abnormal accumulation in the centrosomal area. If this be the case in the motor neuron, a large proportion of damaged mitochondria could be targeted to the cell body in a slow process leading to the accumulation of vacuolated mitochondria in the cell perikaryon.

Taken together, our observations further emphasize the importance of the axonal compartment in ALS, as suggested in the dying-back model of progression of the disease (13). In this regard, it was observed that SOD1 can be synthesized in axons (34, 38). This may result in local accumulation of misfolded mutant SOD1 in the axonal compartment. Further characterization of early axonal SOD1 homeostasis and mitochondrial dysfunction could establish new therapeutic targets and may contribute to understanding the nature and relevance of distal axonal degeneration in ALS.

Acknowledgments

We thank the Department of Proteins and Nucleic Acids and the confocal microscopy core of the IIBCE for their support. Thanks to Pak Chan for the wtSOD-expressing rats. This work was funded by ALSA grant 963 and PEW Latin American Fellowship in Biomedical Sciences, to Jose Sotelo, and in part by Uruguayan agencies like CSIC, PDT-CONICYT, and PEDECIBA. Part of this work was made possible by access to the Cell Imaging and Analysis Core of the NIEHS Core Center (ES00240) and support from grants NS058628 and AT002034. Special thanks to Pablo Diaz and Andres de Leon for genotyping animals used in this study.

JRSS performed research for Figs. 2–9; JRSS and LB designed research; PL and VE contributed to Figs. 2, 6, 8, and 9; LMP contributed to Fig. 7; SH, FP, and MM performed research for Fig. 1; JSB contributed to Fig. 4; JRSS, JSB, and LB analyzed data and wrote the article.

Abbreviations

ALS, amyotrophic lateral sclerosis; CVIP, complex five inhibitory protein; nNOS, neuronal nitric oxide synthase; SOD1, superoxide dismutase-1.

Author Disclosure Statement

No competing financial interests exist.

References

1. Abe K, Pan LH, Watanabe M, Kato T, and Itoyama Y. Induction of nitrotyrosine-like immunoreactivity in the lower motor neuron of amyotrophic lateral sclerosis. *Neurosci Lett* 199: 152–154, 1995.
2. Alvarez B, Demicheli V, Duran R, Trujillo M, Cervenansky C, Freeman BA, and Radi R. Inactivation of human Cu,Zn superoxide dismutase by peroxynitrite and formation of histidinyl radical. *Free Radic Biol Med* 37: 813–822, 2004.
3. Andersen PM. Genetics of sporadic ALS. *Amyotroph Lateral Scler Other Motor Neuron Disord* 2(suppl 1): S37–S41, 2001.
4. Basso M, Massignan T, Samengo G, Cheroni C, De Biasi S, Salmona M, Bendotti C, and Bonetto V. Insoluble mutant SOD1 is partly oligoubiquitinated in amyotrophic lateral sclerosis mice. *J Biol Chem* 281: 33325–33335, 2006.
5. Beckman JS, Estevez AG, Crow JP, and Barbeito L. Superoxide dismutase and the death of motoneurons in ALS. *Trends Neurosci* 24: S15–S20, 2001.
6. Bruijn LI, Beal MF, Becher MW, Schulz JB, Wong PC, Price DL, and Cleveland DW. Elevated free nitrotyrosine levels, but not protein-bound nitrotyrosine or hydroxyl radicals, throughout amyotrophic lateral sclerosis (ALS)-like disease implicate tyrosine nitration as an aberrant in vivo property of one familial ALS-linked superoxide dismutase 1 mutant. *Proc Natl Acad Sci U S A* 94: 7606–7611, 1997.

7. Bruijn LI, Miller TM, and Cleveland DW. Unraveling the mechanisms involved in motor neuron degeneration in ALS. *Annu Rev Neurosci* 27: 723–749, 2004.
8. Cheroni C, Peviani M, Cascio P, Debiasi S, Monti C, Bendotti C. Accumulation of human SOD1 and ubiquitinated deposits in the spinal cord of SOD1G93A mice during motor neuron disease progression correlates with a decrease of proteasome. *Neurobiol Dis* 18: 509–522, 2005.
9. Costes SV, Daelemans D, Cho EH, Dobbin Z, Pavlakis G, and Lockett S. Automatic and quantitative measurement of protein-protein colocalization in live cells. *Biophys J* 86: 3993–4003, 2004.
10. Craig AM and Banker G. Neuronal polarity. *Annu Rev Neurosci* 17: 267–310, 1994.
11. De Vos KJ, Chapman AL, Tennant ME, Manser C, Tudor EL, Lau KF, Brownlees J, Ackerley S, Shaw PJ, McLoughlin DM, Shaw CE, Leigh PN, Miller CC, and Grierson AJ. Familial amyotrophic lateral sclerosis-linked SOD1 mutants perturb fast axonal transport to reduce axonal mitochondria content. *Hum Mol Genet* 16: 2720–2728, 2007.
12. Dupuis L, Gonzalez de Aguilar JL, Oudart H, de Tapia M, Barbeito L, and Loeffler JP. Mitochondria in amyotrophic lateral sclerosis: a trigger and a target. *Neurodegener Dis* 1: 245–254, 2004.
13. Fischer LR, Culver DG, Tennant P, Davis AA, Wang M, Castellano-Sanchez A, Khan J, Polak MA, and Glass JD. Amyotrophic lateral sclerosis is a distal axonopathy: evidence in mice and man. *Exp Neurol* 185: 232–240, 2004.
14. Gal J, Strom AL, Kilty R, Zhang F, and Zhu H. p62 Accumulates and enhances aggregate formation in model systems of familial amyotrophic lateral sclerosis. *J Biol Chem* 282: 11068–11077, 2007.
15. Gurney ME, Pu H, Chiu AY, Dal Canto MC, Polchow CY, Alexander DD, Caliendo J, Hentati A, Kwon YW, Deng HX, Chen W, Zhai P, Sufit RL, and Siddique T. Motor neuron degeneration in mice that express a human Cu,Zn superoxide dismutase mutation. *Science* 264: 1772–1775, 1994.
16. Hirano A, Nakano I, Kurland LT, Mulder DW, Holley PW, and Saccomanno G. Fine structural study of neurofibrillary changes in a family with amyotrophic lateral sclerosis. *J Neuropathol Exp Neurol* 43: 471–480, 1984.
17. Howland DS, Liu J, She Y, Goad B, Maragakis NJ, Kim B, Erickson J, Kulik J, DeVito L, Psaltis G, DeGennaro LJ, Cleveland DW, and Rothstein JD. Focal loss of the glutamate transporter EAAT2 in a transgenic rat model of SOD1 mutant-mediated amyotrophic lateral sclerosis (ALS). *Proc Natl Acad Sci U S A* 99: 1604–1609, 2002.
18. Johnston JA, Dalton MJ, Gurney ME, and Kopito RR. Formation of high molecular weight complexes of mutant Cu, Zn-superoxide dismutase in a mouse model for familial amyotrophic lateral sclerosis. *Proc Natl Acad Sci U S A* 97: 12571–12576, 2000.
19. Koenig E. Isolation of native Mauthner cell axoplasm and an analysis of organelle movement in non-aqueous and aqueous media. *Brain Res* 398: 288–297, 1986.
20. Koenig E, Martin R, Titmus M, and Sotelo-Silveira JR. Cryptic peripheral ribosomal domains distributed intermittently along mammalian myelinated axons. *J Neurosci* 20: 8390–8400, 2000.
21. Koenig E and Repasky E. A regional analysis of alpha-spectrin in the isolated Mauthner neuron and in isolated axons of the goldfish and rabbit. *J Neurosci* 5: 705–714, 1985.
22. Kong J and Xu Z. Massive mitochondrial degeneration in motor neurons triggers the onset of amyotrophic lateral sclerosis in mice expressing a mutant SOD1. *J Neurosci* 18: 3241–3250, 1998.
23. Liu J, Lillo C, Jonsson PA, Vande Velde C, Ward CM, Miller TM, Subramaniam JR, Rothstein JD, Marklund S, Andersen PM, Brännström T, Gredal O, Wong PC, Williams DS, and Cleveland DW. Toxicity of familial ALS-linked SOD1 mutants from selective recruitment to spinal mitochondria. *Neuron* 43: 5–17, 2004.
24. Lobsiger CS, Garcia ML, Ward CM, and Cleveland DW. Altered axonal architecture by removal of the heavily phosphorylated neurofilament tail domains strongly slows superoxide dismutase 1 mutant-mediated ALS. *Proc Natl Acad Sci U S A* 102: 10351–10356, 2005.
25. McAuliffe MJ LF, McGarry D, Gandler W, Csaky K, and Trus BL. Medical image processing, analysis and visualization in clinical research. *IEEE Comput-Based Med Syst (CBMS)* 5: 381–386, 2001.
26. Miller KE and Sheetz MP. Axonal mitochondrial transport and potential are correlated. *J Cell Sci* 117: 2791–2804, 2004.
27. Pasinelli P, Belford ME, Lennon N, Bacskai BJ, Hyman BT, Trotti D, and Brown RH Jr. Amyotrophic lateral sclerosis-associated SOD1 mutant proteins bind and aggregate with Bcl-2 in spinal cord mitochondria. *Neuron* 43: 19–30, 2004.
28. Rosen DR, Siddique T, Patterson D, Figlewicz DA, Sapp P, Hentati A, Donaldson D, Goto J, O'Regan JP, Deng HX, Rahmani Z, Krizus A, McKenna-Yasek D, Cayabyab A, Gaston SM, Berger R, Tanzi R, Halperin JJ, Herzfeldt B, Van den Bergh R, Hung WY, Bird T, Deng G, Mulder DW, Smyth C, Laing NG, Soriano E, Pericak-Vance M, Haines J, Rouleau G, Gusella JS, Horvitz HR, and Brown RH. Mutations in Cu/Zn superoxide dismutase gene are associated with familial amyotrophic lateral sclerosis. *Nature* 362: 59–62, 1993.
29. Rouleau GA, Clark AW, Rooke K, Pramatarova A, Krizus A, Suchowersky O, Julien JP, and Figlewicz D. SOD1 mutation is associated with accumulation of neurofilaments in amyotrophic lateral sclerosis. *Ann Neurol* 39: 128–131, 1996.
30. Sasaki S, Warita H, Abe K, and Iwata M. Impairment of axonal transport in the axon hillock and the initial segment of anterior horn neurons in transgenic mice with a G93A mutant SOD1 gene. *Acta Neuropathol* (Berl) 110: 48–56, 2005.
31. Shaw BF and Valentine JS. How do ALS-associated mutations in superoxide dismutase 1 promote aggregation of the protein? *Trends Biochem Sci* 32: 78–85, 2007.
32. Sotelo-Silveira J, Crispino M, Puppo A, Sotelo JR, and Koenig E. Myelinated axons contain beta-actin mRNA and ZBP-1 in periaxoplasmic ribosomal plaques and depend on cyclic AMP and F-actin integrity for in vitro translation. *J Neurochem* 104: 545–557, 2008.
33. Sotelo-Silveira JR, Calliari A, Cardenas M, Koenig E, and Sotelo JR. Myosin Va and kinesin II motor proteins are concentrated in ribosomal domains (periaxoplasmic ribosomal plaques) of myelinated axons. *J Neurobiol* 60: 187–196, 2004.
34. Sotelo-Silveira JR, Calliari A, Kun A, Koenig E, and Sotelo JR. RNA trafficking in axons. *Traffic* 7: 508–515, 2006.
35. Vande Velde C, Miller TM, Cashman NR, and Cleveland DW. Selective association of misfolded ALS-linked mutant SOD1 with the cytoplasmic face of mitochondria. *Proc Natl Acad Sci U S A* 105: 4022–4027, 2008.
36. Williamson TL, Bruijn LI, Zhu Q, Anderson KL, Anderson SD, Julien JP, and Cleveland DW. Absence of neurofilaments

reduces the selective vulnerability of motor neurons and slows disease caused by a familial amyotrophic lateral sclerosis-linked superoxide dismutase 1 mutant. *Proc Natl Acad Sci U S A* 95: 9631–9636, 1998.
37. Williamson TL and Cleveland DW. Slowing of axonal transport is a very early event in the toxicity of ALS-linked SOD1 mutants to motor neurons. *Nat Neurosci* 2: 50–56, 1999.
38. Willis D, Li KW, Zheng JQ, Chang JH, Smit A, Kelly T, Merianda TT, Sylvester J, van Minnen J, and Twiss JL. Differential transport and local translation of cytoskeletal, injury-response, and neurodegeneration protein mRNAs in axons. *J Neurosci* 25: 778–791, 2005.
39. Zhang B, Tu P, Abtahian F, Trojanowski JQ, and Lee VM. Neurofilaments and orthograde transport are reduced in ventral root axons of transgenic mice that express human SOD1 with a G93A mutation. *J Cell Biol* 139: 1307–1315, 1997.

Address reprint requests to:
Jose R. Sotelo-Silveira
Laboratory of Molecular Technology, ATP
SAIC-National Cancer Institute
Frederick, MD

E-mail: soteloj@mail.nih.gov

and

Luis Barbeito
Dept. Cell and Molecular Neurobiology
Instituto de Investigaciones Biologicas Clemente Estable
Montevideo, Uruguay

E-mail: barbeito@pasteur.edu.uy

Date of first submission to ARS Central, April 1, 2009; date of acceptance, April 3, 2009.